

Degenerate cascade fluorescence: Optical spectral-line narrowing via a single microwave cavity

Liang Hu(胡亮), Xiang-Ming Hu(胡响明), and Qing-Ping Hu(胡庆平)

Citation: Chin. Phys. B, 2021, 30 (**6**): 064211. DOI: 10.1088/1674-1056/abd76b
Journal homepage: http://cpb.iphy.ac.cn; http://iopscience.iop.org/cpb

What follows is a list of articles you may be interested in

Resonantly driven exciton Rabi oscillation in single quantum dots emitting at 1300 nm

Yong-Zhou Xue(薛永洲), Ze-Sheng Chen(陈泽升), Hai-Qiao Ni(倪海桥), Zhi-Chuan Niu(牛智川), De-Sheng Jiang(江德生), Xiu-Ming Dou(窦秀明), Bao-Quan Sun(孙宝权)
Chin. Phys. B, 2017, 26 (**8**): 084202. DOI: 10.1088/1674-1056/26/8/084202

Two-dimensional atom localization induced by a squeezed vacuum

Fei Wang(王飞), Jun Xu(徐俊)
Chin. Phys. B, 2016, 25 (**10**): 104201. DOI: 10.1088/1674-1056/25/10/104201

Control of microwave signals using bichromatic electromechanically induced transparency in multimode circuit electromechanical systems

Cheng Jiang(江成), Yuanshun Cui(崔元顺), Xintian Bian(边心田), Xiaowei Li(李晓薇), Guibin Chen(陈贵宾)
Chin. Phys. B, 2016, 25 (**5**): 054204. DOI: 10.1088/1674-1056/25/5/054204

Determination of the atomic density of rubidium-87

Zhao Meng, Zhang Kai, Chen Li-Qing
Chin. Phys. B, 2015, 24 (**9**): 094206. DOI: 10.1088/1674-1056/24/9/094206

Observation of linewidth narrowing due to a spontaneously generated coherence effect

Tian Si-Cong, Wang Chun-Liang, Kang Zhi-Hui, Yang Xiu-Bin, Wan Ren-Gang, Zhang Xiao-Jun, Zhang Hang, Jiang Yun, Cui Hai-Ning, Gao Jin-Yue
Chin. Phys. B, 2012, 21 (**6**): 064206. DOI: 10.1088/1674-1056/21/6/064206

Degenerate cascade fluorescence: Optical spectral-line narrowing via a single microwave cavity*

Liang Hu(胡亮), Xiang-Ming Hu(胡响明)†, and Qing-Ping Hu(胡庆平)

College of Physical Science and Technology, Central China Normal University, Wuhan 430079, *China*

(Received 23 November 2020; revised manuscript received 19 December 2020; accepted manuscript online 30 December 2020)

For a three-level atom, two nondegenerate (even microwave and optical) electric dipole transitions are usually allowed; for either of these, the fluorescence spectra are well-described in terms of spontaneous transitions from a triplet of dressed sublevels to an adjacent lower-lying triplet. When the three dressed sublevels are equally spaced from each other, a remarkable feature known as degenerate cascade fluorescence takes place, which displays a five-peaked structure. We show that a single cavity can make all the spectral lines extremely narrow, whether they arise from cavity-coupled or cavity-free transitions. This effect is based on intrinsic cascade lasing feedback and makes it possible to use a single microwave cavity (even a bad cavity) to narrow the spectral lines in the optical frequency regime.

Keywords: resonance fluorescence, narrow spectral lines, microwave cavity

PACS: 42.50.Gy, 32.80.Bx **DOI:** 10.1088/1674-1056/abd76b

1. Introduction

Recently, in the manipulation of fluorescence radiation, attention has been paid to the narrowing of spectral lines.[1–25] This will have wide application in improving the accuracy and efficiency of high-precision measurements. The resonant fluorescence of an atom is well described in terms of dressed states, which are degeneracy-lifted composite states of the atom and the dressing fields due to their interaction. As a basic model, for a two-level atom, fluorescence is emitted from a doublet to an adjacent lower-lying doublet.[26] A particularly interesting mechanism for achieving spectral narrowing is to tune a resonant cavity with an inverted dressed-state subtransition and to create a dressed-state laser.[27–37] The essential mechanism is cavity feedback into the fluorescence emission dynamics.

In this paper, we reveal a unique feature that occurs when the cavity-feedback mechanism is applied to a three-level atom, in which two allowed electric dipole transitions, located respectively within the microwave and optical frequency regimes, are linked to a common level. This configuration of interaction is absent for the two-level atom, because a single transition is only within either microwave or the optical regime, but not both. This is unique, because a single microwave cavity can be used to narrow all optical spectral lines. Fluorescence is emitted from a triplet to an adjacent lower-lying triplet.[38–42] Degenerate cascade fluorescence appears when the three dressed states are equally spaced from each other. A single microwave cavity that resonates with the cascade-dressed transitions is sufficient to make each dressed state enter the cavity-feedback dynamic, which gives rise to the narrowing of spectral lines from optical transitions. The novelty of the generalization from the two- to three-level atomic system lies in two aspects, as follows.

First, fluorescence emission occurs from a dressed triplet to the lower adjacent triplet, and generally exhibits a seven-peaked structure. With equal spacing between adjacent sublevels, the fluorescence spectrum takes on a five-peaked structure and cascade degenerate fluorescence happens. The essential difference, compared with the case of the two-level atom, is the equal spacing of the adjacent dressed states, which determines the existence of the degenerate cascade fluorescence. We now focus on the structure of cascade degenerate fluorescence and consider the effect of the intrinsic cascade lasing feedback on the representative fluorescence spectra when a single cavity is tuned to be resonant with the inverted dressed transition. The lasing oscillation happens in a predictable regime only when the light amplification by the inverted dressed transition dominates, compared to the light absorbed by the uninverted dressed transition. Due to the simultaneous interactions, one- and two-photon coherences are simultaneously established between the triplet of dressed states. It is such coherences of the dressed atomic states that cause the five spectral lines from one triplet to the adjacent lower triplet to be extremely narrow and high, while, as described in previous works, narrowing only occurs at the central peak or peaks either side.

Second, since the degenerate cascade laser is sufficient for the narrowing of all spectral lines, whether from a cavity-coupled trasition or a cavity-free optical transition, a microwave cavity (even a bad cavity) can be used to narrow the optical spectral lines from the cavity-free transi-

*Project supported by the National Natural Science Foundation of China (Grants Nos. 61875067 and 61178021).

†Corresponding author. E-mail: xmhu@mail.ccnu.edu.cn

© 2021 Chinese Physical Society and IOP Publishing Ltd

tion. This has been a specific long-term aim for atom–photon interactions.[43–46] Unlike the two-level atom case, where a single transition is either in the microwave regime or in the optical regime, the three-level atom has two cascade transitions that belong to different regimes, e.g., the former is in the microwave regime and the latter is in the optical regime. Because of the existence of a triplet of dressed states for a driven three-level atom, more often than not, degenerate dressed-state transitions have no global population inversion. That is, one dressed-state transition with population inversion is connected to another transition without inversion. Lasing without inversion provides an efficient mechanism for cavity-feedback dynamics.

Our scheme should be distinguished from two other kinds of three-level atomic system. One type of scheme is based on atom–cavity dynamics below the lasing threshold.[22,24] In this case, there is no lasing oscillation, even if population inversion is present. One cavity can only make two dressed states enter the atomic dynamic. More dressed states need more cavities, and thus the experimental difficulty is greatly increased. The other type of scheme is based on parallel dipole moments.[10–13] The requirements of this kind of scheme are too stringent, due to the limitations imposed by selection rules. Even an equivalent realization in dressed-state representation is not enough to avoid the strict requirements of the parallel dipole moments,[47,48] because inherent spontaneous emission of the involved control transitions itself becomes an additional obstacle that is difficult to overcome, and negates the desirable coherent effects.

The remaining part of this paper is organized as follows. In Section 2, we first present the representative fluorescence spectrum of a three-level atom without a cavity and give the locations of the spectral lines in terms of dressed atomic states. Then, in Section 3, we describe dressed-state lasing without global population inversion when the three-level atom interacts with a cavity. We include the Hamiltonian for the dressed-state laser, the possible regimes for laser gain, and the steady-state laser intensity. The main results and the underlying physics are described in Section 4. Finally, we give a summary in Section 5.

2. Representative structure of a fluorescence spectrum in free space

Our purpose is to study the fluorescence spectrum of a three-level atom that interacts with two strong dressing fields plus a weak cavity field. To study cavity effects, we select a structure representative of a fluorescence spectrum in free space, because the spectrum generally has a fairly complicated dependence on the dressing fields.[38–41] While the strong dressing fields define the entire spectral structure, the weak cavity field affects the widths and heights of the spectral lines. For a three-level atom, as shown in Fig. 1, we focus on a equally spaced five-peaked structure (Fig. 3), which appears when the atom is dressed by two dressing fields with equal Rabi frequencies and opposite detunings. We use $|1,2\rangle$ to denote the two ground states and $|3\rangle$ stands for the excited state. We use $2\Omega_{1,2}$ to denote the real Rabi frequencies of the interactions of the two driving fields of circular frequencies $\omega_{1,2}$ with the atom on the $|1,2\rangle \leftrightarrow |3\rangle$ transitions, respectively. The master equation for the density operator ρ of the atom-field system is written in the dipole approximation and in an appropriate rotating frame as

$$\dot{\rho} = -\frac{\mathrm{i}}{\hbar}[H_0, \rho] + \mathcal{L}\rho, \tag{1}$$

where the Hamiltonian

$$H_0 = \hbar \sum_{l=1,2} [-\Delta_l \sigma_{ll} + \Omega_l(\sigma_{l3} + \sigma_{3l})] \tag{2}$$

describes the interaction of the atom with the dressing fields. $\hbar$ is the Planck constant, $\sigma_{kl} = |k\rangle\langle l|$ $(k,l = 1,2,3)$ are the atomic flip spin $(k \neq l)$ and projection $(k = l)$ operators, and $\Delta_l = \omega_{3l} - \omega_l$ $(l = 1,2)$ are the detunings of the applied driving fields from the atomic resonance frequencies. The damping term in the master equation is written[2–7]

$$\mathcal{L}\rho = \sum_{l=1,2} \frac{\gamma_{l3}}{2} \mathcal{L}_{\sigma_{l3}}\rho, \tag{3}$$

where $\mathcal{L}_{\sigma_{l3}}\rho$ describes the atomic decay at a rate of γ_{l3}, and takes the standard form $\mathcal{L}_o\rho = 2o\rho o^\dagger - o^\dagger o\rho - \rho o^\dagger o$, $o = \sigma_{l3}$, $l = 1,2$. In this article, we focus on the spectral structure under the conditions of equal Rabi frequencies and the opposite detunings

$$\Omega_1 = \Omega_2 = \Omega, \quad \Delta_1 = -\Delta_2 = -\Delta, \tag{4}$$

and we describe the Rabi frequencies, the circular frequencies, and the damping rates in units of $\gamma_{l3} = \gamma$. After diagonalizing the Hamiltonian H_0, we obtain the dressed states, which are expressed in terms of the bare atomic states as[7]

$$\begin{aligned}
|+\rangle &= \frac{1+\sin\theta}{2}|1\rangle + \frac{1-\sin\theta}{2}|2\rangle + \frac{\cos\theta}{\sqrt{2}}|3\rangle,\\
|0\rangle &= -\frac{\cos\theta}{\sqrt{2}}|1\rangle + \frac{\cos\theta}{\sqrt{2}}|2\rangle + \sin\theta|3\rangle,\\
|-\rangle &= \frac{1-\sin\theta}{2}|1\rangle + \frac{1+\sin\theta}{2}|2\rangle - \frac{\cos\theta}{\sqrt{2}}|3\rangle,
\end{aligned} \tag{5}$$

where we define $\cos\theta = \sqrt{2}\Omega/d$ and $\sin\theta = \Delta/d$. These dressed states $|0\rangle$ and $|\pm\rangle$ have their eigenvalues $E_{0,\pm} = 0, \pm\hbar d$, which are indeed equally spaced. The dressed-state transitions are shown in Fig. 2(a). For cascaded transitions, we easily find that the degenerate transitions $|+\rangle \leftrightarrow |0\rangle \leftrightarrow |-\rangle$ exist for a degenerate two-photon process, as shown in Fig. 2(b). The free Hamiltonian H_0 for the dressed atom now becomes $H_0 = \hbar d(\sigma_{++} - \sigma_{--})$. We further assume that the general-

ized Rabi frequency $d=\sqrt{2\Omega^2+\Delta^2}$ is much stronger than the atomic relaxation rate, $d\gg\gamma$. Following the standard technique, working in the dressed-state representation, we derive the Bloch equations as follows:

$$\begin{aligned}
\langle\dot{\sigma}_{0+}\rangle &= -\Gamma_1\langle\sigma_{0+}\rangle+\Gamma_2\langle\sigma_{-0}\rangle,\\
\langle\dot{\sigma}_{-0}\rangle &= -\Gamma_1\langle\sigma_{-0}\rangle+\Gamma_2\langle\sigma_{0+}\rangle,\\
\langle\dot{\sigma}_{-+}\rangle &= -\Gamma_3\langle\sigma_{-+}\rangle,\\
\langle\dot{\sigma}_{++}\rangle &= -\gamma_1\langle\sigma_{++}\rangle+\gamma_2\langle\sigma_{--}\rangle+\gamma_3\langle\sigma_{00}\rangle,\\
\langle\dot{\sigma}_{--}\rangle &= -\gamma_1\langle\sigma_{--}\rangle+\gamma_2\langle\sigma_{++}\rangle+\gamma_3\langle\sigma_{00}\rangle,
\end{aligned}\tag{6}$$

together with the closure relation $\sigma_{++}+\sigma_{00}+\sigma_{--}=1$ and the equations for $\sigma_{lk}^{*}=\sigma_{kl}$ $(k\neq l;\, l,k=0,\pm)$. Here, we have defined the decay rates $\Gamma_1=\frac{\gamma}{2}(2-\cos^4\theta)$, $\Gamma_2=\frac{\gamma}{2}\cos^2\theta\sin^2\theta$, $\Gamma_3=\frac{\gamma}{4}(4\cos^2\theta+\cos^4\theta)$, $\gamma_1=\frac{\gamma}{4}(2\cos^2\theta+\cos^4\theta)$, $\gamma_2=\frac{\gamma}{4}(1-\sin^4\theta)$, and $\gamma_3=\frac{\gamma}{2}(\sin^2\theta+\sin^4\theta)$.

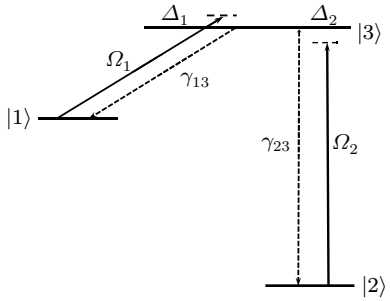


Fig. 1. Schematic diagram for a three-level atom that has two spontaneous transitions $|3\rangle\rightsquigarrow|1\rangle$ and $|3\rangle\rightsquigarrow|2\rangle$ (with rates of γ_{13} and γ_{23}, respectively) in a Λ configuration that interacts with two dressing fields with Rabi frequencies $\Omega_{1,2}$ and detunings $\Delta_{1,2}$, respectively.

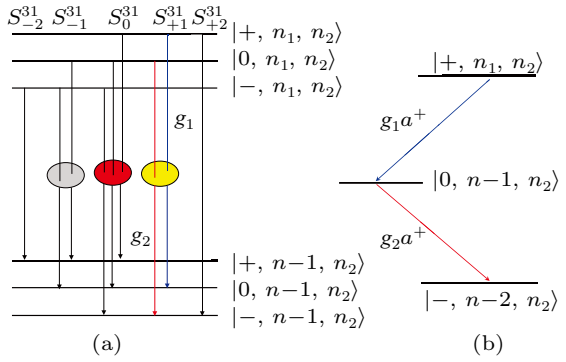


Fig. 2. (a) A pictorial representation of the dressed transitions that are contained in one spontaneous transition, e.g, $|3\rangle\rightsquigarrow|1\rangle$. The dressed transitions occur from a triplet to its lower adjacent triplet. The vertical lines through a common disc correspond to the same sidebands. S^{31}_{+1} and S^{31}_{-1} are two pairs of degenerate cascade fluorescence. (b) A cavity is set up to resonate with the transitions denoted by the red and blue lines in (a). The interaction of the dressed atom with a cavity field is established through degenerate cascade dressed-state transitions $|+,n_1,n_2\rangle\leftrightarrow|0,n_1-1,n_2\rangle\leftrightarrow|-,n_1-2,n_2\rangle$.

We obtain the steady-state populations $\bar{z}_{0,1,2}$ (where the bar "$-$" over z denotes the steady state) of $|0\rangle,|+\rangle,|-\rangle$ as

$$\bar{z}_0=\frac{\cos^4\theta}{1+3\sin^4\theta},\quad \bar{z}_{1,2}=\frac{1}{2}(1-\bar{z}_0).\tag{7}$$

Once $\Delta=0$, i.e., $\sin\theta=0$, $\cos\theta=1$, we have $\bar{z}_0=1$, $\bar{z}_{1,2}=0$. This indicates that the atom is trapped in the dark state.[42] Here, we focus on the case of $\Delta\neq0$, where the atom is excited when $|\Delta|\lesssim\Omega$. By arranging the expectation values into a column vector $X(t)=(\langle\sigma_{+-}\rangle,\langle\sigma_{+0}\rangle,\langle\sigma_{-0}\rangle,\langle\sigma_{++}\rangle,\langle\sigma_{--}\rangle,\langle\sigma_{0-}\rangle,\langle\sigma_{0+}\rangle,\langle\sigma_{-+}\rangle)^{\mathrm{T}}$, we write the equation of motion in the compact form

$$\dot{X}(t)=-QX(t)+M,\tag{8}$$

where the matrix Q is easily obtained from equation (6), and M is the inhomogeneous term $M=(0,\,0,\,0,\,\gamma_3,\,\gamma_3,0,0,0)^{\mathrm{T}}$. The two-time correlation-function matrix $S(\tau)=\langle\delta X(t+\tau)\delta X^{\mathrm{T}}(t)\rangle$ can be calculated using the quantum regression theorem.[1–7] The two-time correlation $S(\tau)$ satisfies the same equation of motion as the one-time average $X(t)$ with a vanishing inhomogeneous term

$$\frac{\mathrm{d}}{\mathrm{d}\tau}S=-QS.\tag{9}$$

Using the Laplace transform $S(\omega)=\frac{1}{\sqrt{2\pi}}\int_{-\infty}^{+\infty}\mathrm{e}^{\mathrm{i}\omega\tau}S(\tau)\mathrm{d}\tau$, we obtain the correlation spectrum matrix

$$S(\omega)=(Q+\mathrm{i}\omega I)^{-1}S(0),\tag{10}$$

where we have used $S(0)=\langle\delta X(t)\delta X^{\mathrm{T}}(t)\rangle_{t\to\infty}$ and an identity matrix I.

The incoherent part of the fluorescence spectrum spontaneously emitted by the $|3\rangle\rightsquigarrow|l\rangle$ $(l=1,2)$ transition is defined as[2–7]

$$S^{3l}(\omega)=\mathrm{Re}\int_0^{\infty}\mathrm{e}^{\mathrm{i}(\omega-\omega_l)\tau}\mathrm{d}\tau\langle\delta\sigma_{3l}(t+\tau)\delta\sigma_{l3}(t)\rangle_{t\to\infty}.\tag{11}$$

Reversing Eq. (5), we express the fluorescence spectrum in terms of the dressed states as

$$\begin{aligned}
S^{3l}(\omega) \;=\; &\mathrm{Re}[R_1^lS_{44}(\tilde{\omega}_0)+R_1^{l+1}S_{55}(\tilde{\omega}_0)+R_2S_{45}(\tilde{\omega}_0)\\
&+R_2S_{54}(\tilde{\omega}_0)+R_3S_{27}(\tilde{\omega}_{-1})+R_4^lS_{63}(\tilde{\omega}_{-1})\\
&+R_5^lS_{23}(\tilde{\omega}_{-1})+R_5^lS_{67}(\tilde{\omega}_{-1})+R_3S_{36}(\tilde{\omega}_{+1})\\
&+R_4^{l+1}S_{72}(\tilde{\omega}_{+1})+R_5^{l+1}S_{76}(\tilde{\omega}_{+1})+R_5^{l+1}S_{32}(\tilde{\omega}_{+1})\\
&+R_6^lS_{18}(\tilde{\omega}_{-2})+R_6^{l+1}S_{81}(\omega_{+2})],
\end{aligned}\tag{12}$$

where the elements $S_{ij}(\omega)$ of the correlation matrix S in equation (10) are used, the frequency arguments

$$\tilde{\omega}_k=\omega-\omega_l-kd\quad(l=1,2;k=0,\pm1,\pm2)\tag{13}$$

are defined, and the R parameters are listed in Appendix C. By $\tilde{\omega}_k=0$, we have five spectral peaks at $\omega=\omega_l+kd$ $(k=0,\pm1,\pm2)$ for the transitions $|3\rangle\rightsquigarrow|l\rangle$ $(l=1,2)$. The sum of the four terms $S_0^{3l}(\omega)=\mathrm{Re}[R_1^lS_{44}(\tilde{\omega}_0)+R_1^{l+1}S_{55}(\tilde{\omega}_0)+R_2S_{45}(\tilde{\omega}_0)+R_2S_{54}(\tilde{\omega}_0)]$ gives the central peak at $\omega=\omega_l$. It originates from the spontaneous emissions $|+\rangle\rightsquigarrow|+\rangle$, $|-\rangle\rightsquigarrow|-\rangle$, and $|0\rangle\rightsquigarrow|0\rangle$. It is described by the self- and cross-correlations of two projection operators $\sigma_{\pm\pm}$, as shown in Eq. (6), since $\sigma_{++}+\sigma_{00}+\sigma_{--}=1$ is satisfied. The sum of the four terms $S_{-1}^{3l}(\omega)=\mathrm{Re}[R_3S_{27}(\tilde{\omega}_{-1})+R_4^lS_{63}(\tilde{\omega}_{-1})+R_5^lS_{23}(\tilde{\omega}_{-1})+R_5^lS_{67}(\tilde{\omega}_{-1})]$ corresponds to the

lower-frequency inner peak at $\omega = \omega_l - d$. It is based on the spontaneous emissions $|0\rangle \rightsquigarrow |+\rangle$ and $|-\rangle \rightsquigarrow |0\rangle$. It is determined by the self- and cross-correlations of the spin operators σ_{0+} and σ_{-0}. The sum of the four terms $S^{3l}_{+1}(\omega) = \mathrm{Re}[R_3 S_{36}(\tilde{\omega}_{+1}) + R_4^{l+1} S_{72}(\tilde{\omega}_{+1}) + R_5^{l+1} S_{76}(\tilde{\omega}_{+1}) + R_5^{l+1} S_{32}(\tilde{\omega}_{+1})]$ describes the higher-frequency inner peak at $\omega = \omega_l + d$. It depends on the spontaneous emissions $|+\rangle \rightsquigarrow |0\rangle$ and $|0\rangle \rightsquigarrow |-\rangle$. It is expressed by the self- and cross-correlations of the spin operators σ_{+0} and σ_{0-}. Finally, $S^{3l}_{-2}(\omega) = \mathrm{Re}[R_6^l S_{18}(\tilde{\omega}_{-2})]$ and $S^{3l}_{+2}(\omega) = \mathrm{Re}[R_6^{l+1} S_{81}(\omega_{+2})]$ stand for the outermost lower- and higher-frequency peaks, respectively, and originate from the spontaneous emissions $|-\rangle \rightsquigarrow |+\rangle$ and $|+\rangle \rightsquigarrow |-\rangle$, respectively. They are caused by the self-correlations of the spin operators σ_{+-} and σ_{-+}. As an example, the five components $S^{31}_0(\omega)$, $S^{31}_{+1}(\omega)$, $S^{31}_{-1}(\omega)$, $S^{31}_{+2}(\omega)$, $S^{31}_{-2}(\omega)$ of the fluorescence spectrum $S^{31}(\omega)$ are labeled in Figs. 2(a) and 3. Meanwhile, the analytical solutions for $S^{3l}_k(\omega)$ are given in Appendix C.

Figure 3 is a plot of the total spectrum for the spontaneous emission of a single transition $|3\rangle \rightsquigarrow |1\rangle$ for $\Delta/\Omega = 1.5$. The spectrum displays asymmetry for a dressing-field frequency of $\omega = \omega_1$. This is because, for transitions at symmetric frequencies, the dressed states $|\pm\rangle$ have the same populations [see Eq. (7)], but their involved dressed-state transitions have completely different coupling strengths [see Eqs. (18) and (19)]. However, because of the symmetrically opposite detunings $\Delta_1 = -\Delta_2 = \Delta \neq 0$, a symmetry exists between the fluorescence spectra from the two wings $S^{31}(\omega)$ and $S^{32}(\omega)$. If the atomic ground states $|1,2\rangle$ are degenerate and the fluorescence takes the form $S^{31}(\omega) + S^{32}(\omega)$, it turns out to be symmetric with the central frequency.

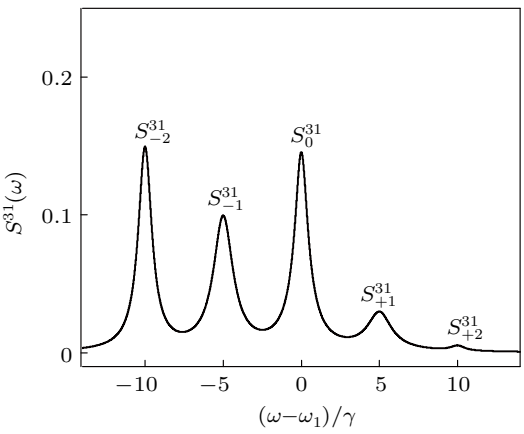


Fig. 3. Representative five-peaked spectrum $S^{31}(\omega)$ of spontaneous emission from the $|3\rangle \rightsquigarrow |1\rangle$ transition of a three-level Λ atom in free space. Equal Rabi frequencies and opposite detunings are chosen, $\Omega = 5\gamma/2$ and $\Delta = 5\gamma/\sqrt{2}$ ($\Delta/\Omega = \sqrt{2} > 1$), such that we have $d = \sqrt{2\Omega^2 + \Delta^2} = 5\gamma$. The five peaks are located at $(\omega - \omega_2)/\gamma = 0, \pm 5, \pm 10$.

Our focus is on the nondegenerate case and to show the cavity-feedback mechanism and conditions for the narrowing of all spectral lines in Fig. 3. The essential difference, compared to the case of the two-level atom, is the equal spacing of the adjacent dressed states, which determines the existence of a pair of degenerate cascade transitions, e.g., $|+,n_1,n_2\rangle \rightarrow |0,n_1-1,n_2\rangle$ and $|0,n_1,n_2\rangle \rightarrow |-,n_1-1,n_2\rangle$. Actually, this corresponds to the degenerate two-photon process $|+,n_1,n_2\rangle \rightarrow |0,n_1-1,n_2\rangle \rightarrow |-,n_1-2,n_2\rangle$. The cavity feedback is simply based on a single-mode dressed laser generated by the system itself. This is different from cases that use external fields such as the squeezed or thermal vacuum fields, as in Refs. [49,50].

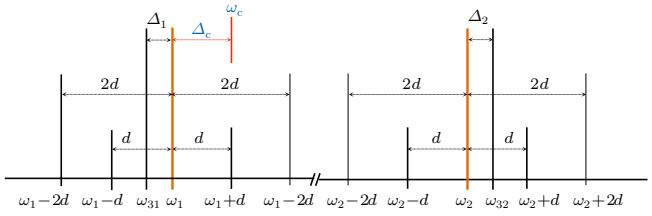


Fig. 4. Diagrammatic sketch for various frequencies and detunings along the frequency axis. The left and right parts, which center at the dressing field frequencies $\omega_{1,2}$ respectively, are related to the dipole-allowed transitions $|1\rangle \leftrightarrow |3\rangle$ and $|2\rangle \leftrightarrow |3\rangle$ respectively. The dressing field frequencies $\omega_{1,2}$ are very close to ω_{31} and ω_{32} by the detunings $\Delta_{1,2}$, respectively. The five peaks locate at ω_l, $\omega_l \pm d$, $\omega_l \pm 2d$ ($l = 1,2$), respectively. The cavity field is tuned to be resonant with the upper inner sideband of the $|1\rangle \leftrightarrow |3\rangle$ transition, $\omega_c = \omega_1 + d$, i.e., $\Delta_c = d$.

3. Dressed-state lasing without global population inversion

After having chosen the representative spectral structure of the three-level atom in free space, we turn to a consideration of cavity-feedback effects. For this purpose, in addition to the interaction of the atom with the dressing fields, we need to include the interaction of the atom with the cavity field in the system dynamics. While the interaction with the dressing fields is merged into the dressed atomic states, the interaction with the cavity field is analyzed in terms of the dressed states.

3.1. Interaction of CPT atom with a cavity field

We assume that a cavity field of frequency ω_c is coupled to a wing of the Λ configuration, e.g., the $|1\rangle \leftrightarrow |3\rangle$ transition. The Hamiltonian for the interaction of the cavity field with the atom is written in the rotating frame as[2–7]

$$H_I = \hbar\Delta_c a^\dagger a + \hbar g(a\sigma_{31} + \sigma_{13}a^\dagger). \tag{14}$$

The cavity mode, which is described by the annihilation and creation operators a and $a^\dagger$, is detuned from the driving field by $\Delta_c = \omega_c - \omega_1$. The strength of the atom–cavity field coupling is g. We define the operators $\sigma_{kl} = |k\rangle\langle l|$ and $l,k = 1-3$ for the bare atomic states and $l,k = 0$ and $\pm$ for the dressed atomic states are the spin-flip ($k \neq l$) and projection ($k = l$) operators. The master equation for the density operator ρ of the atom–field system takes the conventional form[3]

$$\dot{\rho} = -\frac{\mathrm{i}}{\hbar}[H_0 + H_I, \rho] + \mathcal{L}\rho, \tag{15}$$

where H_0 is in the same form as that shown for Eq. (2), except that the collective atomic operators are substituted for one-atom operators, and the atomic and cavity relaxations are contained in $\mathcal{L}\rho = \kappa\mathcal{L}_a\rho + \sum_{l=1,2}\frac{\gamma_{l3}}{2}\mathcal{L}_{\sigma_{l3}}\rho$, where the cavity and atomic decay rates are 2κ and γ_{l3}, respectively.

We tune the cavity field resonant with two degenerate dressed transitions $|+\rangle \leftrightarrow |0\rangle$ and $|0\rangle \leftrightarrow |-\rangle$, from which the atom emits fluorescent photons at the higher inner sidebands

$$\Delta_c = d, \tag{16}$$

as shown in Fig. 2(a) by the two vertical lines (red and blue) surrounded by the yellow circle. The case $\Delta_c = -d$ is treated in the same way. To clearly compare the frequencies involved and the detunings, we list them along a frequency axis in Fig. 4. In our calculation, we have taken equal Rabi frequencies and the opposite detunings, as shown in Eq. (4). We assume the cavity field to have a small Rabi frequency $\Omega_\alpha = g\langle a\rangle$ (real) and a small damping rate

$$d \gg \Omega_\alpha, \kappa, \tag{17}$$

and make a further unitary transformation with the free parts for the dressed atom and the cavity field $H_0 + \hbar\Delta_c a^\dagger a$. After performing the transformation, we obtain the interaction Hamiltonian

$$\tilde{H}_I = \hbar g_1(a\sigma_{+0} + \sigma_{0+}a^\dagger) + \hbar g_2(a\sigma_{0-} + \sigma_{-0}a^\dagger), \tag{18}$$

where $g_{1,2}$ are the effective coupling strengths

$$g_1 = -\frac{1}{2}g\cos^2\theta, \quad g_2 = \frac{1}{2}g\sin\theta(1-\sin\theta). \tag{19}$$

It can clearly be seen from the Hamiltonian (18) that the cavity field a is in simultaneous resonance with two individual transitions $|+\rangle \leftrightarrow |0\rangle$ and $|0\rangle \leftrightarrow |-\rangle$, as shown in Fig. 2(b). Not only are there two one-photon processes for the individual transitions, but also two-photon process happens for the following transition $|+\rangle \leftrightarrow |0\rangle \leftrightarrow |-\rangle$. Once the cavity field a is amplified above the threshold, one- and two-photon coherences are established between the dressed atomic states. The coherences have significant effects on the fluorescence spectrum, depending on the coupled dynamics of the cavity field and the dressed atom. In what follows, we will show that the fluorescence spectrum is indeed remarkably modified under appropriate conditions. In particular, the coherences induce the narrowing of the spectral lines, both from the cavity-coupled bare-state transition $|3\rangle \rightsquigarrow |1\rangle$, and from the non-cavity-coupled bare-state transition $|3\rangle \rightsquigarrow |2\rangle$. In the following three subsections, we describe the dressed-state laser gain, calculate the steady-state laser intensity, and present the coherence between the dressed states.

3.2. Linear gain without global population inversion

Dressed-state lasers are a special kind of system, which are driven by strong external coherent fields.[27–37] The degenerate composite states of the atom plus the dressing fields are lifted into the dressed states, which are shifted by the generalized Rabi frequency d from the dressing-field frequencies. Population inversion is established for one of shifted transitions between adjacent dressed-state triplets, depending on the dressing-field Rabi frequencies $\Omega_{1,2} = \Omega$ and detunings $\Delta_{1,2} = \mp\Delta$. Dressed-state inversion is used to create the laser gain. The essential difference from the previous dressed-state lasers is that the laser oscillation is created from a degenerate cascade of two dressed-state transitions, $|+\rangle \leftrightarrow |0\rangle$ and $|0\rangle \leftrightarrow |-\rangle$, and one two-photon process, $|+\rangle \leftrightarrow |0\rangle \leftrightarrow |-\rangle$. The onset of the dressed-state laser is described by the linear gain, which only depends on the one-photon processes. The two-photon transition is involved only when the saturation behavior is considered.

In this subsection, we first focus on the onset of the dressed-state laser. The linear gain for the laser amplitude $\langle a\rangle$ can be obtained from Eq. (24) or (26), and is given below, following Refs. [1–7]:

$$G(0) = \frac{\Gamma_1}{\Gamma_1^2 - \Gamma_2^2}(g_1^2 - g_2^2)(\bar{z}_1 - \bar{z}_0), \tag{20}$$

where, for the two decay rates, $\Gamma_1 > \Gamma_2$, and have used the average populations $\bar{z}_0$ and $\bar{z}_1 = \bar{z}_2$ per atom in Eq. (7). The dressed-state population inversion $z = \bar{z}_1 - \bar{z}_0 > 0$ is always accompanied by noninversion $\bar{z}_0 - \bar{z}_2 = -z < 0$, and vice visa. This is the so-called "without global population inversion". It is clear that the linear gain, which is based on the two degenerate dressed-state transitions, has a more complicated dependence on the normalized detuning Δ/Ω. In particular, it depends on the difference of the effective coupling strength squares $g_1^2 - g_2^2$. If we define the Δ/Ω-dependent cooperativity parameters for the two transitions $\tilde{C}_l = g_l^2\Gamma_1/[\kappa(\Gamma_1^2 - \Gamma_2^2)]$, the conditions for the amplification of the cavity field below or above the threshold are

$$\begin{aligned} &0 < (\tilde{C}_1 - \tilde{C}_2)z < 1 \quad \text{below the threshold,} \\ &(\tilde{C}_1 - \tilde{C}_2)z > 1 \quad \text{above the threshold,} \end{aligned} \tag{21}$$

where z is the unsaturated population difference. The difference $\tilde{C}_1 - \tilde{C}_2$ of the cooperativity parameters arises from the opposite contributions of the two degenerate dressed-state transitions $|+\rangle \leftrightarrow |0\rangle$ and $|0\rangle \leftrightarrow |-\rangle$. One contribution is proportional to $\bar{z}_1 - \bar{z}_0 > 0$, while the other is determined by $\bar{z}_0 - \bar{z}_2 < 0$ ($\bar{z}_2 = \bar{z}_1$). The linear gain is positive ($G(0) > 0$) only when the conditions $g_1^2 > g_2^2$ and $\bar{z}_1 > \bar{z}_0$ are simultaneously satisfied, or when the conditions are simultaneously changed to $g_1^2 < g_2^2$ and $\bar{z}_1 < \bar{z}_0$. The dependence of the population difference has been given in Eq. (7). The effective coupling strengths have a dependence on Δ/Ω as follows:

$$\begin{aligned} &|g_1| > |g_2| \quad \text{for} \quad \Delta/\Omega < -\sqrt{2/3}, \\ &|g_1| < |g_2| \quad \text{for} \quad \Delta/\Omega > -\sqrt{2/3}. \end{aligned} \tag{22}$$

By analysis, we can identify the four regimes in which both the dressed populations and the effective coupling strengths have different dependences on the normalized detuning. For clarity, we present the regimes in Table 1. We can see in which regime dressed-state lasing is possible.

(i) For $\Delta/\Omega < -1$, we have the relations for populations where $\bar{z}_{1,2} > \bar{z}_0$ and for the effective coupling strengths, where $|g_1|^2 < |g_2|^2$. The amplification due to the $|+\rangle \leftrightarrow |0\rangle$ transition is weaker than the absorption from the $|0\rangle \leftrightarrow |-\rangle$ transition. No net gain happens and no lasing action happens.

(ii) For $-1 < \Delta/\Omega < -\sqrt{2/3}$, the dressed populations are reversed, $\bar{z}_{1,2} < \bar{z}_0$, and the effective coupling strengths maintain the relation $|g_1|^2 < |g_2|^2$. The amplification from the $|0\rangle \leftrightarrow |-\rangle$ transition dominates, compared to the absorption from the $|+\rangle \leftrightarrow |0\rangle$ transition. A net gain is apparent and lasing is possible.

(iii) For $-\sqrt{2/3} < \Delta/\Omega < 0$ and $0 < \Delta/\Omega < 1$, the population continues to satisfy the relation, $\bar{z}_{1,2} < \bar{z}_0$ and the effective coupling strengths reverse their relation, $|g_1|^2 > |g_2|^2$. The absorption from the $|+\rangle \leftrightarrow |0\rangle$ transition dominates, compared to the amplification from the $|0\rangle \leftrightarrow |-\rangle$ transition. Consequently, the net gain disappears and no lasing occurs.

(iv) For $\Delta/\Omega > 1$, the population relation is reversed once again $\bar{z}_{1,2} > \bar{z}_0$ and the coupling strengths comply with $|g_1|^2 > |g_2|^2$. The amplification from the $|+\rangle \leftrightarrow |0\rangle$ transition becomes dominant compared to the absorption from the $|0\rangle \leftrightarrow |-\rangle$ transition. Once again, a net gain exists and lasing is achievable.

To sum up, lasing oscillation is possible in the two different regimes: $\Delta/\Omega = (-1, -\sqrt{2/3})$ and $(1, +\infty)$. Only in these two regimes does the cavity field obtain a nonzero amplitude and feed back into the atom.

On the other hand, in the same way we can give the possible parameter regimes for $\Delta_c = -d$. The onset of the cavity field is determined by the linear gain based on the one-photon processes caused by degenerate cascade transitions $|-\rangle \leftrightarrow |0\rangle$ and $|0\rangle \leftrightarrow |+\rangle$. The linear gain becomes

$$G(0) = \frac{\Gamma_1}{\Gamma_1^2 - \Gamma_2^2}(g_1^2 - g_2^2)(\bar{z}_0 - \bar{z}_1). \tag{23}$$

The possible parameter regimes for dressed-state lasing are changed to different regimes, as given in Table 2.

Table 1. Possible regimes of parameters for dressed-state laser oscillation in the higher sideband $\Delta_c = d$.

Ranges of normalized detuning Δ/Ω	i$(-\infty,-1)$	ii$(-1,-\sqrt{2/3})$	iii$(-\sqrt{2/3},0),(0,1)$	iv$(1,\infty)$
Dressed-state populations	$\bar{z}_{1,2} > \bar{z}_0$	$\bar{z}_{1,2} < \bar{z}_0$	$\bar{z}_{1,2} < \bar{z}_0$	$\bar{z}_{1,2} > \bar{z}_0$
Effective coupling strengths	$\|g_1\| < \|g_2\|$	$\|g_1\| < \|g_2\|$	$\|g_1\| > \|g_2\|$	$\|g_1\| > \|g_2\|$
Linear gain	$G(0) < 0$	$G(0) > 0$	$G(0) < 0$	$G(0) > 0$
Dominant processes	Absorption	Amplification	Absorption	Amplification
Possibility of dressed-state lasing	No	Possible	No	Possible

Table 2. Possible regimes of parameters for dressed-state laser oscillation at lower sideband $\Delta_c = -d$.

Ranges of normalized detuning Δ/Ω	i$(-\infty,-1)$	ii$(-1,-\sqrt{2/3})$	iii$(-\sqrt{2/3},0),(0,1)$	iv$(1,\infty)$
Dressed-state populations	$\bar{z}_{1,2} > \bar{z}_0$	$\bar{z}_{1,2} < \bar{z}_0$	$\bar{z}_{1,2} < \bar{z}_0$	$\bar{z}_{1,2} > \bar{z}_0$
Effective coupling strengths	$\|g_1\| < \|g_2\|$	$\|g_1\| < \|g_2\|$	$\|g_1\| > \|g_2\|$	$\|g_1\| > \|g_2\|$
Linear gain	$G(0) > 0$	$G(0) < 0$	$G(0) > 0$	$G(0) < 0$
Dominant processes	Amplification	Absorption	Amplification	Absorption
Possibility of dressed-state lasing	Possible	No	Possible	No

3.3. Steady-state laser intensity

We are now in a position to include the nonlinear effects of the dressed-state laser. To do so, we have to calculate the intensity of the dressed-state laser. This is a necessary step for calculating the cavity-modified fluorescence spectrum. The strong dressing fields, the amplitudes of which are given initially, are assumed not to change during the interaction and are merged into the atomic dressed states. However, the cavity field, which is created via the degenerate cascade quantum transitions, has an unknown amplitude. Only when the cavity field amplitude is obtained can we have the steady-state solutions of the populations and polarizations of the dressed atom, and we can then derive the cavity- mediated fluorescence spectrum. Since we focus on the case close to the threshold, the cavity field will be much weaker than the dressing fields, $\Omega_\alpha \ll \Omega$. In this case, it will not be convenient to use the cavity field to redress the atom. Instead, it is most convenient for us to follow the standard methods,[2–5] where the dressed states are determined only by the strong dressing fields. For the present system, while the five-peaked structure of the fluorescence spectrum is determined by the dressing fields, the narrowing of all five peaks is based on the interaction of the generated cavity fields with the dressed atoms. Although the dressing fields and the cavity fields are coexistent, the present system is confined to the weak cavity fields, i.e., $g^2 I = \Omega_\alpha^2 \ll |\Omega|^2$, as shown below in Fig. 5. This guarantees that the present dressed-state approach holds good.

To obtain the cavity field intensity and further to probe its effects on the fluorescence spectrum, we have to solve the master equation (15) for the reduced density operator. To do so, we have to arrange the atomic and field operators involved into a definite sequence and collect the additional terms that origi-

nate from the operator commutation relations. This technique is well established in books.[2–5] By treating the quantum-mechanical operators as the corresponding c-numbers, we can transform the master equation into a set of derivative equations of c-numbers. By doing so, we preserve the classical and quantum statistical properties, including the classical (mean) behavior and the quantum-noise properties. To the usual second order, we have Langevin equations (equivalent to a Fokker–Planck equation).

To transform to the c-number representation, we choose the normal ordering (σ_{+-}, σ_{+0}, σ_{-0}, σ_{++}, σ_{--}, σ_{0-}, σ_{0+}, σ_{-+}, $a^\dagger$, a), and define the corresponding c-number correspondences (υ_3^*, υ_1^*, υ_2, z_1, z_2, υ_2^*, υ_1, υ_3, α^*, α). The set of Heisenberg–Langevin equations is derived as

$$\begin{aligned}
\dot{\alpha} &= -\kappa\alpha - \mathrm{i}g_1\upsilon_1 - \mathrm{i}g_2\upsilon_2 + F_\alpha,\\
\dot{\upsilon}_1 &= -\Gamma_1\upsilon_1 + \Gamma_2\upsilon_2 + \mathrm{i}g_1\alpha(z_1 - z_0) + \mathrm{i}g_2\alpha^*\upsilon_3 + F_{\upsilon_1},\\
\dot{\upsilon}_2 &= -\Gamma_1\upsilon_2 + \Gamma_2\upsilon_1 + \mathrm{i}g_2\alpha(z_0 - z_2) - \mathrm{i}g_1\alpha^*\upsilon_3 + F_{\upsilon_2},\\
\dot{\upsilon}_3 &= -\Gamma_3\upsilon_3 - \mathrm{i}g_1\alpha\upsilon_2 + \mathrm{i}g_2\alpha\upsilon_1 + F_{\upsilon_3},\\
\dot{z}_1 &= -\gamma_1 z_1 + \gamma_2 z_2 + \gamma_3 z_0 - \mathrm{i}g_1(\alpha\upsilon_1^* - \alpha^*\upsilon_1) + F_{z_1},\\
\dot{z}_2 &= -\gamma_1 z_2 + \gamma_2 z_1 + \gamma_3 z_0 + \mathrm{i}g_2(\alpha\upsilon_2^* - \alpha^*\upsilon_2) + F_{z_2};
\end{aligned} \tag{24}$$

together with the complex conjugates and the closure relation $z_0 + z_1 + z_2 = 1$. F's are white noises, which have the vanishing means and nonvanishing second-order correlations listed in Appendix B.

We see from Eq. (24) that the cavity field amplitude α, the atomic polarizations $\upsilon_{1,2,3}$ and the atomic populations $z_{1,2}$ are strongly coupled with each other. The first equation in which two atomic polarizations $\upsilon_{1,2}$ (one-photon coherences) simultaneously contribute to the the cavity field is that for α. This originates from the degenerate cascade interactions of the dressed atom with the cavity field. The second and third equations show that $\upsilon_{1,2}$ are created, respectively, due to atomic population differences $(z_{1,2} - z_0)$ and coupled to the third polarization υ_3 (two-photon coherence) via the cavity field α. The fourth equation shows that the atomic polarization υ_3 is supported by two atomic polarizations $\upsilon_{1,2}$. The last two equations reflect the nonlinear couplings of the populations to the cavity field α via the atomic polarizations $\upsilon_{1,2}$. The absorptive, dispersive and fluorescent responses of the dressed atom to the intracavity field can be obtained from the set of nonlinearly coupled equations.

We can derive an equation of motion for the cavity field α by temporarily neglecting the noise and setting the atomic derivatives to zero. First, we express υ_{1-3} in terms of the populations z_{0-2} from a closed set of equations for υ_{1-3}. We then use υ_{1-3} to solve for z_{0-2}, and insert z_{0-2} back into the expressions of υ_{1-3}. Finally, substituting $\upsilon_{1,2}$ into the equation for α yields

$$\dot{\alpha} = (G - \kappa)\alpha \tag{25}$$

with a nonlinear gain of

$$G(I) = \frac{A_0 + A_1 I + A_2 I^2}{K_0 + K_1 I + K_2 I^2 + K_3 I^3}, \tag{26}$$

where we have defined the photon number $I = \langle\alpha^*\alpha\rangle$, and have listed the A's and K's parameters in Appendix A. The nonlinear gain $G(I)$ is simply reduced to the linear gain $G(0)$ in Eq. (20) when $I = 0$. The explicit expression for the laser gain clearly displays deep nonlinearities based on the degenerate two-photon process. Except for the complicated dependence of parameters, the A_0 and $K_{0,1}$ terms originate from the two degenerate one-photon transitions $|+\rangle \leftrightarrow |0\rangle$ and $|0\rangle \leftrightarrow |-\rangle$. The $A_{1,2}$ and $K_{2,3}$ terms are due to the two-photon process $|+\rangle \leftrightarrow |0\rangle \leftrightarrow |-\rangle$, as shown in Fig. 3(b), which is absent in the two-level system.[15,16,23,27–30] When the linear laser gain satisfies the different conditions

$$\begin{aligned}
&0 < G(0) < \kappa \quad \text{below threshold},\\
&G(0) > \kappa \quad \text{above threshold},
\end{aligned} \tag{27}$$

the cavity field has a different behavior. The cavity field has a zero mean below the threshold, $\bar{\alpha} = 0$ and a nonvanishing mean $\bar{\alpha} \neq 0$ above the threshold. The latter is the case in which a dressed-state lasing oscillation is created. In the steady state, we can solve for the photon number $\bar{I}$ by setting $\dot{\alpha} = 0$. These steady-state solutions are given in Appendix A. Stability is guaranteed by the term $\mathrm{d}G(I)/\mathrm{d}I|_{I=\bar{I}} < 0$. This only holds for the adiabatic case ($\kappa \ll \gamma_{1-3}, \Gamma_{1-3}$). However, we are not confined to the adiabatic case. Beyond the adiabatic conditions, stability is guaranteed by requiring positive eigenvalues of the drift matrix B that will appear in Eq. (28) below. This corresponds to the requisite condition that any variable has to keep its fluctuation evolution below the threshold, even when it is amplified. The curves in Fig. 5 from bottom to top correspond to the laser intensity $g^2\bar{I}$ for $C = g^2/(\kappa\gamma) = 60$ (dotted), 64 (dashed), and 68 (solid) and $\kappa = 5\gamma$. This figure verifies the light amplification in regime IV, as listed in Table 1. It can be seen that the cavity field Rabi frequency $\Omega_\alpha = g\bar{\alpha} = g\sqrt{\bar{I}} < \gamma$, which indicates that the cavity field does not yield further splitting of the dressed states. It is for this reason that we use the dressed states only by means of the strong dressing fields. At this stage, a dressed atom behaves in the same way as a normal bare atom and interacts with the cavity field.

Once the mean field amplitude is obtained, we can easily derive from Eq. (24) the steady-state solutions of the average per atom $\bar{\upsilon}_{1-3}$ and $\bar{z}_{0-2}^{\mathrm{c}}$, which are listed in Appendix A, and in which the superscript "c" denotes the saturated values in the presence of the nonvanishing cavity field as distinguished from those of the vanishing cavity field. The nonlinearity of the cavity field is fed back to the dressed atom itself and has remarkable effects on the fluorescence spectrum.

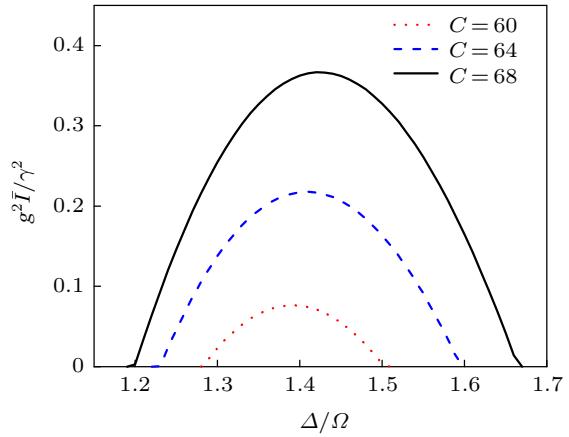


Fig. 5. The intensity $g^2\bar{I}/\gamma^2$ of the dressed-state laser above threshold versus the normalized detuning Δ/Ω for $\kappa = 5\gamma$ and $C = 60$ (dotted), 64 (dashed), and 68 (solid).

4. Extreme narrowing for an entire five-peaked structure

So far, we have calculated the intensities of the dressed laser and presented a numerical verification of the establishment of weak coherence in the dressed state. In this section, we derive the cavity-mediated fluorescence spectrum and physically analyse the effects of weak coherence on the spectral lines.

4.1. Cavity feedback mediated spectrum

Having obtained the cavity field amplitude and the atomic populations and polarizations, we can proceed to the inclusion of quantum noises, F's, and the derivation of the correlation spectrum, which is common to the absorptive and dispersive response of the dressed atom to the intracavity field, and also common to the transmitted and fluorescent light.[51–53] The incoherent fluorescent light emitted perpendicular to the direction of the cavity field propagation is shown in Eq. (11). To obtain the total spectrum, we need to calculate those spectra that come from the dressed transitions. The cavity-feedback-based spectra are obtained from the set of Heisenberg–Langevin equations (24) by following the standard techniques.[2–6,51–53] Performing linearization on Eq. (24) and arranging the corresponding quantities in exactly the same order as $X(t)$ in section two, plus the laser fields $\delta O(t) = \delta(\upsilon_3^*, \upsilon_1^*, \upsilon_2, z_1, z_2, \upsilon_2^*, \upsilon_1, \upsilon_3, \alpha^*, \alpha,)^{\mathrm{T}}$ and $F(t) = (F_{\upsilon_3^*}, F_{\upsilon_1^*}, F_{\upsilon_2}, F_{z_1}, F_{z_2}, F_{\upsilon_2^*}, F_{\upsilon_1}, F_{\upsilon_3}, F_{\alpha^*}, F_{\alpha})^{\mathrm{T}}$, we derive a set of linearized Heisenberg–Langevin equations in a compact form

$$\frac{\mathrm{d}}{\mathrm{d}t}\delta O(t) = -B\delta O(t) + F(t), \tag{28}$$

where the drift matrix B is easily obtained from Eq. (24). Stability is guaranteed by keeping all eigenvalues of the drift matrix B positive. The noise correlation is derived from the Einstein relation[2–6], $\langle F(t)F^{\mathrm{T}}(t')\rangle = D\delta(t-t')$, where the nonvanishing elements of diffusion matrix D are listed in the Appendix B. Using the Fourier transformation $\delta O(\omega) = \frac{1}{\sqrt{2\pi}}\int_{-\infty}^{+\infty} \mathrm{e}^{\mathrm{i}\omega t}\delta O(t)\mathrm{d}t$, we obtain the fluctuation correlation spectrum matrix

$$\langle \delta O(\omega)\delta O(\omega')\rangle = S(\omega)\delta(\omega+\omega'), \tag{29}$$

where $S(\omega)$ is in a 10×10 matrix form

$$S(\omega) = (B + \mathrm{i}\omega I)^{-1} D (B^{\mathrm{T}} - \mathrm{i}\omega I)^{-1}. \tag{30}$$

The elements $S_{kl}(\omega)$ $(k,l = 1-8)$ give the atomic correlations with the cavity feedback included. Substituting the elements of $S_{kl}(\omega)$ into Eq. (12), we obtain the fluorescence spectra from the transitions $|3\rangle \rightsquigarrow |1\rangle$ and $|3\rangle \rightsquigarrow |2\rangle$ of the three-level atom in a cavity.

4.2. Complete narrowing for $S^{31}(\omega)$ from cavity-mediated transition

After obtaining the fluorescence spectra from the cavity-coupled and non-cavity-coupled transitions of the three-level atom, we present the main results and the underlying physics. In Fig. 6, the spectrum $S^{31}(\omega)$ is plotted for the cavity-coupled transition $|3\rangle \rightsquigarrow |1\rangle$ when the cavity field is amplified above threshold. The parameters chosen are $C = 60$, $d = 5\gamma$, $\kappa = 5\gamma$ (Fig. 6).

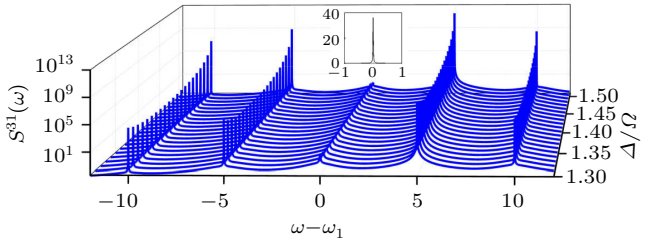


Fig. 6. Fluorescence spectra for the $|3\rangle \rightsquigarrow |1\rangle$ transition of a dressed three-level atom in a cavity above threshold ($G(0) > \kappa$). The parameters used are $C = 60$, $\kappa = 5\gamma$, and $d = 5\gamma$. We fix $d = 5\gamma$ to avoid an overlap of the spectral peaks. The insert uses a linear coordinate for the central peak. Narrowing happens for all five peaks.

In Fig. 7 the spectrum $S^{32}(\omega)$ is plotted for the non-cavity-coupled transition $|3\rangle \rightsquigarrow |2\rangle$ for the same parameters as in Fig. 6. In all these figures, we fix $d = 5\gamma$ to avoid an overlap of the spectral peaks. The spectra $S^{31}(\omega)$ and $S^{32}(\omega)$ have essentially the same structures and features under the same conditions, although the cavity is only coupled to the $|3\rangle \rightsquigarrow |1\rangle$ transition but not to the $|3\rangle \rightsquigarrow |2\rangle$ transition. The spectral lines from the $|3\rangle \rightsquigarrow |l\rangle$ transition are located at the center $\omega = \omega_l$, at the inner sidebands $\omega = \omega_l \pm d$, and at the outermost sidebands $\omega = \omega_l \pm 2d$ $(l = 1, 2)$.

The extremely narrow lines appear within the predicable regimes of the normalized detuning Δ/Ω. Since spectral narrowing is based on dressed-state lasing, the regimes for narrowing are confined to regions II: $\Delta/\Omega = (-1, -\sqrt{2/3})$ and IV: $\Delta/\Omega = (1, \infty)$, as shown in Table 1. First, it is clearly seen from Fig. 6 that the spectral peaks are extremely narrow and high. Although the central peak is much lower than the side

peaks, it is much higher than in the usual case without a cavity. Numerically, the spectral peaks have linewidths of about 1% of the natural atomic linewidths. Second, we note that the cavity is a bad cavity, $\kappa \gg \gamma$, i.e., the spectrum narrowing holds, even for a bad cavity.

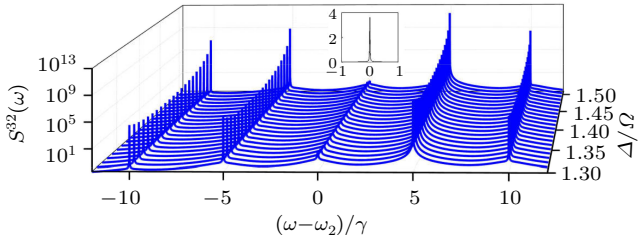


Fig. 7. Fluorescence spectra for the $|3\rangle \rightsquigarrow |2\rangle$ transition of a dressed three-level atom in a cavity above threshold ($G(0) > \kappa$). The parameters are the same as for Fig. 6.

Third, the excitation of the atom and the level splitting are determined by the strong dressing fields, and instead the role of the weak cavity field is that it establishes the weak coherence of the well-separated dressed states. The conditions are summarized as

$$\begin{aligned} &\text{(i)} && \Omega_{1,2} = \Omega, \quad \Delta_{1,2} = \pm\Delta, \quad |\Delta| \sim \Omega, \\ &\text{(ii)} && \Delta_c = d, \quad \text{or} \quad \Delta_c = -d, \\ &\text{(iii)} && d \gg (\Omega_\alpha, \gamma, \kappa). \end{aligned} \tag{31}$$

In the dressed-state picture, the spontaneous transition $|3\rangle \rightsquigarrow |1\rangle$ happens from a triplet to its adjacent triplet $|k, n_1, n_2\rangle \rightsquigarrow |l, n_1 - 1, n_2\rangle$, $k, l = 0, \pm$, respectively. As shown in Fig. 2(b), the two successive degenerate dressed-state transitions $|+\rangle \leftrightarrow |0\rangle$ and $|0\rangle \leftrightarrow |-\rangle$ are in simultaneous resonance with the common cavity field. The cavity field, if it is amplified below threshold, has a vanishing amplitude, and does not induce coherence between the dressed states. The dressed-state laser, once it is created through the cascade transitions $|+\rangle \leftrightarrow |0\rangle$ and $|0\rangle \leftrightarrow |-\rangle$, establishes coherences between the dressed states. The degenerate one-photon transitions $|+\rangle \leftrightarrow |0\rangle$ and $|0\rangle \leftrightarrow |-\rangle$ and the two-photon transition $|+\rangle \leftrightarrow |0\rangle \leftrightarrow |-\rangle$ are coupled to each other. In subsection 3.3, we already obtained the cavity field intensity $g^2\bar{I}$, whose dependence on the normalized detuning is shown in Fig. 5. With the intensity, we also obtained the coherences between the dressed states $\bar{v}_{1-3}$ of the average per atom, which are shown in Fig. 8(a) for the $C = 60, \kappa = 5\gamma$. Because of the one- and two-photon resonances, the polarizations $\bar{v}_{1,2}$ have purely imaginary parts, while the polarization $\bar{v}_3$ is purely real. There are two characteristic features for the cavity-feedback dynamics.

As a first feature, all three dressed states are involved in the cavity feedback dynamics. This is based on the same processes as used for the laser creation. As shown in Fig. 2, the cavity field simultaneously interacts with the two degenerate cascade dressed-state transitions $|+\rangle \leftrightarrow |0\rangle$ and $|0\rangle \leftrightarrow |-\rangle$. Such degeneracy is absent in the most widely studied two-level systems, where the dressed transitions happen from a well-separated doublet to its adjacent lower doublet. For the three-level atom, in sharp contrast, the dressed transitions appear from an equally spaced triplet to its adjacent lower triplet, as shown in Fig. 2(a). Because of the equal spacing, degenerate transitions $|+\rangle \leftrightarrow |0\rangle$ and $|0\rangle \leftrightarrow |-\rangle$ appear in pairs. For three adjacent triplets in the two-dimensional networks of dressed states $|k, n_1, n_2\rangle$ ($k = 0, \pm$), the degenerate transitions combine to support a two-photon process $|+\rangle \leftrightarrow |0\rangle \leftrightarrow |-\rangle$, as shown in Fig. 2(b). It is the two one-photon processes and the two-photon process that determine the dressed atomic polarizations $\upsilon_{1,2,3}$, which are coupled to each other and to the cavity field, as shown in Eq. (24).

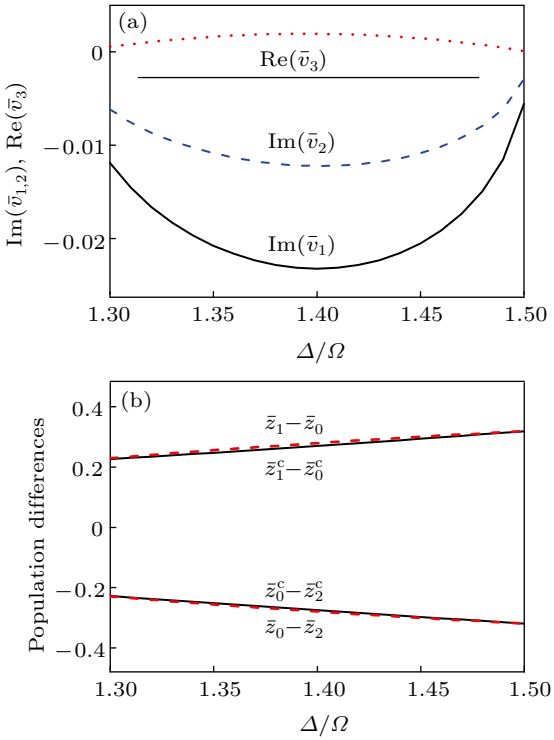


Fig. 8. (a) Dressed-state atomic polarizations for $C = 60, \kappa = 5\gamma$. Note that $\bar{v}_{1,2}$ have purely imaginary components $\mathrm{Im}\,\bar{v}_{1,2}$, while $\bar{v}_3$ only has the real part. (b) A comparison between the saturated population differences $\bar{z}_1^c - \bar{z}_0^c$ and $\bar{z}_0^c - \bar{z}_2^c$ and the unsaturated population differences $\bar{z}_1 - \bar{z}_0$ and $\bar{z}_0 - \bar{z}_2$ for the same parameters as used in (a).

The second feature is that the population inversion of one dressed transition is accompanied by noninversion of the cascaded dressed transition. In the absence of the cavity, we have the unsaturated population differences $\bar{z}_1 - \bar{z}_0 = -(\bar{z}_0 - \bar{z}_2)$. While the inversion of one dressed transition contributes to the laser's linear gain, the noninversion of the other transition reduces the linear gain. As analyzed in Subsection 3.2, a net linear gain is obtained when the coupling strength of the inverted transition dominates, compared to that of the noninverted transition. This determines that the dressed-state laser, even if it is created, is relatively weak. Actually, it is the case, as shown in Fig. 5, that the Rabi frequency $g\bar{\alpha} = g\sqrt{\bar{I}}$ is significantly smaller than the atomic decay rate γ. Such a weak

field hardly modifies the dressed-state populations [Fig. 8(b)], but establishes weak coherences between the dressed states [Fig. 8(a)]. This is in intrinsic agreement with our requirements for a weak cavity field. For the purpose of narrowing the fluorescence spectral lines, the cavity field has to be sufficiently weak to avoid AC Stark splitting and modification of the dressed populations. This guarantees that the spectral lines keep their original locations unchanged when the cavity field induces weak coherences between the dressed states.

As a general principle, the fluctuation spectrum is determined by the behavior of the parts of the coupled system fluctuating around the steady state and below the threshold. The amplification of the fluorescent light field below the threshold should not be confused with the amplification of the cavity field above the threshold. The amplification of the cavity field acting as a dressed-state laser is based on the dominance of the inverted dressed-state transition. The dressed-state laser, after its creation, enters dressed atomic dynamics and mediates the amplification of the fluorescent light below the threshold. In other words, the fluorescence spectrum is determined by the coupled dynamics between the dressed atom and the cavity field. It is easy to deduce that the one- and two-photon coherences of the dressed atomic states will play a crucial role in determining the spectral linewidths and heights.

Spectral line narrowing appears within predictable regimes of the normalized detuning Δ/Ω. The regimes for narrowing are confined to regions II: $\Delta/\Omega = (-1, -\sqrt{2/3})$ and IV: $\Delta/\Omega = (1, \infty)$, as shown in Table 1. As the spontaneous field is amplified below the threshold, this requires that the 10×10 drift matrix B in Eq. (28) has ten positive eigenvalues. In principle, each spectral peak is an incoherent superposition of ten components which are associated with different eigenvalues of B. Stability requires that all eigenvalues of B are positive. One of these ten components is associated with amplification below the threshold. Due to amplification below the threshold, one eigenvalue can be made to approach zero. Once this is the case, the corresponding peak is extremely narrow and high.

4.3. Complete narrowing for $S^{32}(\omega)$ from cavity-free transition

What is most worthwhile to stress is that the cavity field coupled to the $|3\rangle \rightsquigarrow |1\rangle$ transition has remarkable effects on the fluorescence spectral lines of the non-cavity-coupled $|3\rangle \rightsquigarrow |2\rangle$ transition. Figure 7 shows the plotted spectrum $S^{32}(\omega)$ of the atomic transition $|3\rangle \rightsquigarrow |2\rangle$ where the cavity field is amplified above the threshold. It can clearly be seen that the fluorescence spectrum from the non-cavity-coupled $|3\rangle \rightsquigarrow |2\rangle$ transition displays essentially the same structure as that of the cavity-coupled $|3\rangle \rightsquigarrow |1\rangle$ transition. The minor difference lies in the peak heights. For example, there are different heights of the central peaks, as shown in the inserts of Figs. 6 and 7. The spectral narrowing not only happens for the cavity-coupled transition, but also for the non-cavity-coupled transition. When the two wings of the Λ configuration are located in the microwave and the optical regime, respectively, the coupling of the cavity to the microwave transition makes the optical spectral lines extremely narrow. This establishes the possibility of coherent control of optical fields using a microwave cavity. Such a cascade of a microwave transition with an optical transition is most commonly found in various atomic and molecular systems.[43–46,54,55]

It should be emphasized that the spectral line narrowing and heightening are not unbounded, but ultimately limited by quantum fluctuations of the atoms.[3,4,6] Although the dressed-state laser operates near to, and above, the threshold, the linearized system of the atoms and the cavity operates below the threshold. In principle, the linewidths are dependent on all the decay eigenvalues (i.e., the real parts of the eigenvalue of the drift matrix B) of the linearized system, and the extremely narrow linewidth is simply determined by the minimal decay eigenvalue. In the above treatment, the drift matrix B does not, in itself, contain the quantum fluctuations, thus the minimal decay eigenvalue approaches zero and the peak height tends to infinity. Actually, quantum fluctuations should be merged into the drift matrix B. In this case, the minimal decay eigenvalue is roughly estimated to be $\sim \gamma/\sqrt{N}$. For $N \sim 10^8$, we have a minimal linewidth of $\sim 10^{-4}\gamma$, and the maximal peak heights are $\sim 10^4$ times as much as those in free space. Generally speaking, the factors that restrict the lower limit of these linewidths include the dressed-atom–cavity cooperativity parameters, the dressed-state populations and coherences, and the dressed-state laser intensities. As for the dressed atoms, all these factors are strongly dependent on the ratio of the detuning to the Rabi frequency Δ/Ω of the dressing fields.

4.4. Experimental consideration

On the other hand, the present scheme can be generalized to various multilevel systems, typically including those three-level atomic systems in V and ladder configurations. A great number of atomic structures can be used as candidates for the present scheme. For example, the rubidium 85 D_1 transition hyperfine structure (795 nm) is suitable for optical control. The $|1\rangle = |5^2S_{1/2}, F = 1\rangle \leftrightarrow |3\rangle = |5^2P_{1/2}, F = 2\rangle$ transition and the $|2\rangle = |5^2S_{1/2}, F = 2\rangle \leftrightarrow |3\rangle = |5^2P_{1/2}, F = 2\rangle$ transition are in the Λ configuration with two optical transitions. The ground states are separated from each other by 3 GHz and the other excited state hyperfine level $|5^2P_{1/2}, F = 1\rangle$, which is 362 MHz below $|3\rangle$, has a negligible influence. The hydrogen transition hyperfine structure (243 nm) is well suited to microwave control. The $|1\rangle = |2^2S_{1/2}, F = 2\rangle \leftrightarrow |3\rangle = |2^2P_{3/2}, F = 2\rangle$ transition and $|2\rangle = |1^2S_{1/2}, F = 1\rangle \leftrightarrow |3\rangle =$

$|2^2P_{3/2}, F=2\rangle$ transition are in the Λ configuration. The separation between the levels $2^2P_{3/2}$ and $2^2S_{1/2}$ is 9.95 GHZ, corresponding to a microwave transition. Meanwhile, the $|2\rangle = |1^2S_{1/2}, F=1\rangle \leftrightarrow |3\rangle = |2^2P_{3/2}, F=2\rangle$ transition is an optical transition. Thus, we have a cascade of the microwave and optical transitions. So far, there has been great progress in exploring atomic coherence effects induced by microwave fields. Examples include the four-wave mixing of optical and microwave fields in warm rubidium vapor,[43] electromagnetically induced transparency controlled by a microwave field in a dense rubidium gas,[44] and an atomic interface between microwave and optical photons in superconducting resonators, ensembles of ultracold atoms.[45] Progress has also been made with various systems such as ruby,[46] artificial atoms,[54] and molecules (methanol, formaldehyde, ammonia).[55] Therefore, the present scheme is within the reach of current technology.

5. Discussion and conclusions

We should note that the electromagnetically induced transparency (EIT) spectrum is also often chosen to enhance frequency-resolved detection.[56,57] Recently, a proof-of-principle experiment[58] was performed for a superheterodyne receiver based on a microwave-dressed EIT spectrum. The sensitivity was remarkably higher than in previous schemes, such as those based on Autler–Townes splitting or standard atomic electrometers. Although EIT and coherent population trapping can possibly be used to narrow spectral lines, this is usually achieved at the cost of decreasing the power.[59,60] To enhance the accuracy and efficiency of spectra-based high-precision measurements, one expects that the linewidth narrowing of fluorescence spectra should be compatible with spectral heightening. It is clear that the present scheme has the advantage of meeting the above two compatible requirements.

In conclusion, for a three-level atom we have shown that a dressed-state laser from one allowed dipole transition is sufficient to narrow all fluorescence spectral lines. The essential difference from the case of the two-level atom is that the triply degenerate atomic field composite state is lifted as a triplet of equally spaced dressed states. This corresponds to the existence of degenerate dressed-state two-photon transitions, which lead to lasing without global dressed-state population inversion and coupling of all three dressed states to the single-mode cavity field. The required conditions are easily satisfied for a wide range of parameters: symmetric Rabi frequencies and symmetrically opposite detunings. The obtainability of both a single-mode dressed-state laser and its effects show that it is possible to use a microwave cavity to manipulate the fluorescence spectral lines of a cavity-free optical transition in a multilevel atomic system.

Appendix A: Steady-state solutions

We first list the A and K parameters that appear in Eq. (26)

$$
\begin{aligned}
A_0 &= (\gamma_1+\gamma_2)(\gamma_1-\gamma_2-\gamma_3)(g_1^2-g_2^2)\Gamma_1\Gamma_3^2(\Gamma_1^2-\Gamma_2^2),\\
A_1 &= (\gamma_1+\gamma_2)(\gamma_1-\gamma_2-\gamma_3)(g_1^2-g_2^2)\Gamma_3\\
&\quad\times[(g_1^2+g_2^2)(2\Gamma_1^2-\Gamma_2^2)-2g_1g_2\Gamma_1\Gamma_2],\\
A_2 &= (\gamma_1+\gamma_2)(\gamma_1-\gamma_2-\gamma_3)(g_1^4-g_2^4)\\
&\quad\times[(g_1^2+g_2^2)\Gamma_1-2g_1g_2\Gamma_2],
\end{aligned}
$$

and

$$
\begin{aligned}
K_0 &= -(\gamma_1+\gamma_2)(\gamma_1-\gamma_2+2\gamma_3)\Gamma_3^2(\Gamma_1^2-\Gamma_2^2)^2,\\
K_1 &= \{-2(2\gamma_1+\gamma_2+\gamma_3)(g_1^2+g_2^2)\Gamma_1\Gamma_3\\
&\quad+4(\gamma_1+2\gamma_2-\gamma_3)g_1g_2\Gamma_2\Gamma_3-2(\gamma_1+\gamma_2)(\gamma_1-\gamma_2+2\gamma_3)\\
&\quad\times\left[(g_1^2+g_2^2)\Gamma_1-2g_1g_2\Gamma_2\right]\}\Gamma_3(\Gamma_1^2-\Gamma_2^2),\\
K_2 &= 2\left[-(2\gamma_1+\gamma_2+\gamma_3)(g_1^4+g_2^4)+2(\gamma_1+2\gamma_2-\gamma_3+3\Gamma_3)g_1^2g_2^2\right]\\
&\quad\times\Gamma_3(\Gamma_1^2-\Gamma_2^2)\\
&\quad-\left[2(2\gamma_1+\gamma_2+\gamma_3)(g_1^2+g_2^2)\Gamma_1-4(\gamma_1+2\gamma_2-\gamma_3)g_1g_2\Gamma_2\right]\\
&\quad\times\left[(g_1^2+g_2^2)\Gamma_1-2g_1g_2\Gamma_2\right]\Gamma_3\\
&\quad\times-(\gamma_1+\gamma_2)\times(\gamma_1-\gamma_2+2\gamma_3)\left[(g_1^2+g_2^2)\Gamma_1-2g_1g_2\Gamma_2\right]^2,\\
K_3 &= \left[-2(2\gamma_1+\gamma_2+\gamma_3)(g_1^4+g_2^4)+4(\gamma_1+2\gamma_2-\gamma_3+3\Gamma_3)g_1^2g_2^2\right]\\
&\quad\times\left[(g_1^2+g_2^2)\Gamma_1-2g_1g_2\Gamma_2\right].
\end{aligned}
$$

The steady-state laser intensity $\bar{I}$ is then derived as

$$\bar{I} = L_1 + L_2 - L_0,$$

where

$$
\begin{aligned}
L_0 &= E_2/3,\\
L_{1,2} &= \left(-M_1 \pm \sqrt{M_1^2+M_2}\right)^{1/3},\\
M_1 &= (27E_0 - 9E_1E_2 + 2E_2^3)/54,\\
M_2 &= (3E_1 - E_2^2)^3/9^3,\\
E_l &= (\kappa K_l - A_l)/(\kappa K_3), \quad l=0,1,2.
\end{aligned}
$$

Now we present the steady-state solutions for the average $\bar{\upsilon}_{1-3}$ and $\bar{z}^{\rm c}_{0-2}$ per atom, as follows:

$$
\begin{aligned}
\bar{\upsilon}_1 &= \mathrm{i}g_1\bar{\alpha}P_1(\bar{z}_1^{\rm c}-\bar{z}_0^{\rm c}) + \mathrm{i}g_2\bar{\alpha}Q(\bar{z}_0^{\rm c}-\bar{z}_2^{\rm c}),\\
\bar{\upsilon}_2 &= \mathrm{i}g_2\bar{\alpha}P_2(\bar{z}_0^{\rm c}-\bar{z}_2^{\rm c}) + \mathrm{i}g_1\bar{\alpha}Q(\bar{z}_1^{\rm c}-\bar{z}_0^{\rm c}),\\
\bar{\upsilon}_3 &= (-\mathrm{i}g_1\bar{\alpha}\bar{\upsilon}_2 + \mathrm{i}g_2\bar{\alpha}\bar{\upsilon}_1)/\Gamma_3\\
\bar{z}_l^{\rm c} &= D_l/D, \quad l=0,1,2,
\end{aligned}
$$

where

$$
\begin{aligned}
D_0 &= X_{11}X_{22} - X_{21}X_{12},\\
D_1 &= X_{21}X_{13} - X_{11}X_{23},\\
D_2 &= X_{12}X_{23} - X_{22}X_{13},\\
D &= D_0 + D_1 + D_2,\\
X_{11} &= -\gamma_1 - 2g_1^2\bar{I}P_1,\\
X_{12} &= \gamma_2 + 2g_1g_2\bar{I}Q,
\end{aligned}
$$

$$
\begin{aligned}
X_{21} &= \gamma_2 + 2g_1g_2\bar{I}P_2,\\
X_{22} &= -\gamma_1 - 2g_2^2\bar{I}Q,\\
X_{13} &= \gamma_3 + 2g_1^2\bar{I}P_1 - 2g_1g_2\bar{I}Q,\\
X_{23} &= \gamma_3 + 2g_2^2\bar{I}Q - 2g_1g_2\bar{I}P_2,
\end{aligned}
$$

with

$$
\begin{aligned}
P_1 &= (\Gamma_1\Gamma_3 + g_1^2\bar{I})/U,\\
P_2 &= (\Gamma_1\Gamma_3 + g_2^2\bar{I})/U,\\
Q &= (\Gamma_2\Gamma_3 + g_1g_2\bar{I})/U,\\
U &= (\Gamma_1^2 - \Gamma_2^2)\Gamma_3 + (g_1^2 + g_2^2)\bar{I}\Gamma_1 - 2g_1g_2\bar{I}\Gamma_2.
\end{aligned}
$$

Appendix B: The diffusion coefficients

Here, we show the elements of the nonzero diffusion coefficients $D_{oo'}$ in terms of normalized variables. We note that $D_{oo'} = D_{o'o}$ and $D_{o^*o'^*} = D^*_{o'o}$. The nonzero diffusion coefficients are derived as follows:

$$
\begin{aligned}
D_{\alpha z_2} &= -\mathrm{i}g_2\bar{\upsilon}_2,\\
D_{\alpha\upsilon_1} &= \mathrm{i}g_2\bar{\upsilon}_3,\\
D_{\upsilon_2\alpha^*} &= \mathrm{i}g_2(1 - \bar{z}_1^{\mathrm{c}} - 2\bar{z}_2^{\mathrm{c}}),\\
D_{\upsilon_1\upsilon_1} &= 2\mathrm{i}g_1\bar{\alpha}\bar{\upsilon}_1 - 2\Gamma_2\bar{\upsilon}_3,\\
D_{\upsilon_2\upsilon_2} &= -2\mathrm{i}g_2\bar{\alpha}\bar{\upsilon}_2 - 2\Gamma_2\bar{\upsilon}_3,\\
D_{\upsilon_1\upsilon_3} &= \mathrm{i}g_1\bar{\alpha}\bar{\upsilon}_3,\\
D_{\upsilon_2\upsilon_1^*} &= -\mathrm{i}g_1\bar{\alpha}^*\bar{\upsilon}_2 - \Gamma_2(\bar{z}_1^{\mathrm{c}} + \bar{z}_2^{\mathrm{c}}),\\
D_{\upsilon_2\upsilon_3^*} &= -\mathrm{i}g_1\bar{\alpha}^*(\bar{z}_1^{\mathrm{c}} + \bar{z}_2^{\mathrm{c}}) + \mathrm{i}g_2\bar{\alpha}\bar{\upsilon}_3^* + (\Gamma_1 + \Gamma_3)\bar{\upsilon}_1^*,\\
D_{\upsilon_3\upsilon_3^*} &= -\mathrm{i}g_1\bar{\alpha}^*\bar{\upsilon}_1 + \mathrm{i}g_1\bar{\alpha}\bar{\upsilon}_1^* + 2\Gamma_3\bar{z}_1^{\mathrm{c}},\\
D_{\upsilon_1\upsilon_1^*} &= -\mathrm{i}g_1\bar{\alpha}^*\bar{\upsilon}_1 + \mathrm{i}g_1\bar{\alpha}\bar{\upsilon}_1^* + 2\Gamma_1\bar{z}_1^{\mathrm{c}},\\
D_{\upsilon_1\upsilon_3^*} &= -\Gamma_2\bar{\upsilon}_1^*,\\
D_{\upsilon_2\upsilon_2^*} &= (\gamma_1 + \gamma_2)\bar{z}_1^{\mathrm{c}} + (2\Gamma_1 - \gamma_1 - \gamma_2)\bar{z}_2^{\mathrm{c}},\\
D_{\upsilon_1\upsilon_2} &= (2\Gamma_1 - \Gamma_3)\bar{\upsilon}_3,\\
D_{\upsilon_3 z_1} &= -\gamma_2\bar{\upsilon}_3,\\
D_{\upsilon_3 z_2} &= -\mathrm{i}g_2\bar{\alpha}\bar{\upsilon}_1 + (\gamma_1 + \Gamma_3)\bar{\upsilon}_3,\\
D_{\upsilon_1 z_1} &= -\gamma_3\bar{\upsilon}_1,\\
D_{\upsilon_1 z_2} &= -\gamma_3\bar{\upsilon}_1,\\
D_{\upsilon_2 z_1} &= -\mathrm{i}g_1\bar{\alpha}^*\bar{\upsilon}_3 - \gamma_3\bar{\upsilon}_2,\\
D_{\upsilon_2 z_2} &= \mathrm{i}g_1\bar{\alpha}^*\bar{\upsilon}_3 - \gamma_3\bar{\upsilon}_2,\\
D_{z_1 z_1} &= 2\gamma_1\bar{z}_1^{\mathrm{c}},\\
D_{z_1 z_2} &= -\gamma_2(\bar{z}_1^{\mathrm{c}} + \bar{z}_2^{\mathrm{c}}),\\
D_{z_2 z_2} &= 2\gamma_1\bar{z}_2^{\mathrm{c}}.
\end{aligned}
$$

Appendix C: The parameters of the fluorescence spectrum

The parameters R_{1-10} for the fluorescence spectra in Eqs. (12) are shown as follows:

$$
\begin{aligned}
R_1^l &= \frac{1}{8}\cos^2\theta[1 - (-1)^l 3\sin\theta]^2,\\
R_2 &= \frac{1}{8}\cos^2\theta(9\sin^2\theta - 1).\\
R_3 &= \frac{1}{4}\cos^4\theta,\\
R_4^l &= \frac{1}{4}[\sin\theta + (-1)^l\sin^2\theta]^2,\\
R_5^l &= \frac{1}{4}(-1)^l\cos^2\theta[\sin\theta + (-1)^l\sin^2\theta]),\\
R_6^l &= \frac{1}{8}\cos^2\theta[1 + (-1)^l\sin\theta]^2.
\end{aligned}
$$

References

[1] Loudon R 2000 *The Quantum Theory of Light* 3rd ed (Oxford: Oxford University Press)
[2] Walls D F and Milburn G J 2008 *Quantum Optics* 2nd ed (Berlin: Springer-Verlag)
[3] Scully M O and Zubairy M S 1997 *Quantum Optics* (Cambridge: Cambridge University Press)
[4] Gardiner C W and Zoller P 2000 *Quantum Noise* 2nd ed (Berlin: Springer-Verlag)
[5] Carmichael H J 2002 *Statistical Methods in Quantum Optics* 2nd ed (Berlin: Springer)
[6] Meystre P and Sargent III M 2007 *Elements of Quantum Optics* 4th ed (Berlin: Springer-Verlag)
[7] Cohen-Tannoudji C, Dupont-Roc J and Grynberg G 1992 *Atom-photon Interactions* (New York: Wiley)
[8] Boyd R W 2008 *Nonlinear Optics* 3rd ed (New York: Elsevier)
[9] Narducci L M, Scully M O, Oppo G L, Ru P and Tredicce J R R 1990 *Phys. Rev. A* **42** 1630
[10] Zhu S Y, Narducci L M and Scully M O 1995 *Phys. Rev. A* **52** 4791
[11] Agarwal G S 1996 *Phys. Rev. A* **54** R3734
[12] Zhou P and Swain S 1996 *Phys. Rev. Lett.* **77** 3995
[13] Zhou P and Swain S 2000 *Phys. Rev. A* **56** 3011
[14] Keitel C H 1999 *Phys. Rev. Lett.* **83** 1307
[15] Freedhoff H and Quang T 1993 *J. Opt. Soc. Am. B* **10** 1337
[16] Freedhoff H and Quang T 1994 *Phys. Rev. Lett.* **72** 474
[17] Peng J S, Li G X, Zhou P and Swain S 2000 *Phys. Rev. A* **61** 063807
[18] Berman P R 1994 *Cavity Quantum Electrodynamics* (New York: Academic Press)
[19] Kleppner D 1981 *Phys. Rev. Lett.* **47** 233
[20] Goy P, Raimond J M, Gross M and Haroche S 1983 *Phys. Rev. Lett.* **50** 1903
[21] Sanchez-Mondragon J, Narozhny N and Eberly J 1983 *Phys. Rev. Lett.* **51** 550
[22] Haken H 1964 *Z. Phys.* **181** 96
[23] Quang T and Freedhoff H 1993 *Phys. Rev. A* **47** 2285
[24] Huang C, Hu X and Hu Q 2017 *Opt. Express* **26** 4807
[25] Xue Y L, Zhang K, Feng B H and Li Z Y 2016 *Chin. Phys. Lett.* **33** 74204
[26] Mollow B R 1969 *Phys. Rev.* **188** 1969
[27] Mollow B R 1972 *Phys. Rev. A* **5** 2217
[28] Wu F Y, Ezekiel S, Ducloy M and Mollow B R 1977 *Phys. Rev. Lett.* **38** 1077
[29] Khitrova G, Valley J F and Gibbs H M 1988 *Phys. Rev. Lett.* **60** 1126
[30] Mompart J and Corbalán R 2000 *J. Opt. B: Quantum Semiclass. Opt.* **2** R7
[31] Lezama A, Zhu Y, Kanskar M and Mossberg T W 1990 *Phys. Rev. A* **41** 1576
[32] Lewenstein M, Zhu Y and Mossberg T W 1990 *Phys. Rev. Lett.* **64** 3131
[33] Zakrzewski J, Lewenstein M and Mossberg T W 1991 *Phys. Rev. A* **44** 7717
[34] Zakrzewski J, Lewenstein M and Mossberg T W 1991 *Phys. Rev. A* **44** 7732
[35] Zakrzewski J, Lewenstein M and Mossberg T W 1991 *Phys. Rev. A* **44** 7746
[36] Gauthier D J, Wu Q, Morin S E and Mossberg T W 1992 *Phys. Rev. Lett.* **68** 464
[37] Zhu Y, Wu Q, Morin S and Mossberg T W 1990 *Phys. Rev. Lett.* **65** 1200

[38] Lawande S V, D'Souza R and Puri R R 1987 *Phys. Rev. A* **36** 3228
[39] Jayarao A S, Lawande S V and D'Souza R 1989 *Phys. Rev. A* **39** 3464
[40] Gauthier D J, Zhu Y and Mossberg T W 1991 *Phys. Rev. Lett.* **66** 2460
[41] Peng J S and Li G X 1998 *Introduction to modern quantum optics* (Singapore: World Scientific)
[42] Arimondo E 1996 *Prog. Opt.* **35** 257
[43] Zibrov A S, Matsko A B and Scully M O 2002 *Phys. Rev. Lett.* **89** 103601
[44] Li H B, Sautenkov V A, Rostovtsev Y V, Welch G R, Hemmer P R and Scully M O 2009 *Phys. Rev. A* **80** 023820
[45] Hafezi M, Kim Z, Rolston S L, Orozco L A, Lev B L and Taylor J M 2012 *Phys. Rev. A* **85** 020302(R)
[46] Zhao Y, Wu C K,Ham B S, Kim M K and Awad E 1997 *Phys. Rev. Lett.* **79** 641
[47] Fleischhauer M, Keitel C H, Narducci L M, Scully M O, Zhu S Y and Zubairy M S 1992 *Opt. Commun.* **94** 599
[48] Hu X M and Peng J S 2000 *J. Phys. B: At. Mol. Opt. Phys.* **33** 921
[49] Ferguson M, Ficek Z and Dalton B 1996 *Phys. Rev. A* **54** 2379
[50] Macovei M, Evers J and Keitel C H 2004 *Europhys. Lett.* **68** 391
[51] Drummond P D and Walls D F 1981 *Phys. Rev. A* **23** 2563
[52] Carmichael H J, Walls D F, Drummond P D and Hassan S S 1983 *Phys. Rev. A* **27** 3112
[53] Reid M D 1988 *Phys. Rev. A* **37** 4792
[54] Jia W Z, Wei L F and Wang Z D 2011 *Phys. Rev. A* **83** 023811
[55] Scully M O and Zubairy M S 1997 *Quantum Optics* (Cambridge University)
[56] Fleischhauer M, Imamoglu A and Marangos J P 2005 *Rev. Mod. Phys.* **77** 633
[57] Mohapatra A K, Jackson T R and Adams C S 2007 *Phys. Rev. Lett.* **98** 113003
[58] Jing M, Hu Y, Ma J, *et al.* 2020 *Nat. Phys.* **16** 911
[59] Wu Y L, Li R, Rui Y, Jiang H F and Wu H B 2018 *Acta Phys. Sin.* **67** 163201 (in Chinese)
[60] Hao L P, Xue Y M, Fan J B, *et al.* 2020 *Chin. Phys. B* **29** 033201